Dynamics of terraces on a silicon surface due to the combined action of strain and electric current

Wei Hong[a], Zhigang Suo[a,*], Zhenyu Zhang[b,c]

[a]*Division of Engineering and Applied Sciences, Harvard University, Cambridge, MA 02138, USA*
[b]*Materials Science and Technology Division, Oak Ridge National Laboratory, Oak Ridge, TN 37831, USA*
[c]*Department of Physics and Astronomy, The University of Tennessee, Knoxville, TN 37996, USA*

Abstract

A (0 0 1) surface of silicon consists of terraces of two variants, which have an identical atomic structure, except for a $90°$ rotation. We formulate a model to evolve the terraces under the combined action of electric current and applied strain. The electric current motivates adatoms to diffuse by a wind force, while the applied strain motivates adatoms to diffuse by changing the concentration of adatoms in equilibrium with each step. To promote one variant of terraces over the other, the wind force acts on the anisotropy in diffusivity, and the applied strain acts on the anisotropy in surface stress. Our model reproduces experimental observations of stationary states, in which the relative width of the two variants becomes independent of time. Our model also predicts a new instability, in which a small change in experimental variables (e.g., the applied strain and the electric current) may cause a large change in the relative width of the two variants.
© 2007 Elsevier Ltd. All rights reserved.

1. Introduction

The dynamics on crystalline surfaces has long been a subject of basic research. Basic processes include adsorption of atoms, diffusion of adatoms on terraces, and attachment of adatoms to monatomic steps; see Burton et al. (1951), Zhang and Lagally (1997), Pimpinelli and Villain (1998) and Jeong and Williams (1999) for reviews. This paper focuses on the dynamics of terraces on a vicinal (0 0 1) silicon surface, when the crystal is subject to a direct electric current and an applied strain. We formulate a model that reproduces existing experimental observations and predicts an instability that has yet been reported.

As illustrated in Fig. 1, a (0 0 1) surface of silicon is anisotropic. Upon reconstruction, atoms on the surface pair into dimers, which in turn form rows. Along the dimer rows surface stress is compressive and adatoms diffuse fast, while normal to the dimer rows surface stress is tensile and adatoms diffuse slowly (e.g., Alerhand et al., 1988; Mo and Lagally, 1991). Fig. 2 illustrates a surface, vicinal to (0 0 1) and tilted towards [1 1 0],
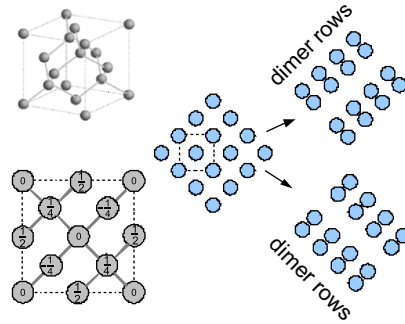

Fig. 1. Silicon has the crystalline structure of diamond. Upon reconstruction, atoms on the surface pair into dimers, which in turn form rows. Depending on the exact atomic plane, the dimer rows can be in either one of two directions.
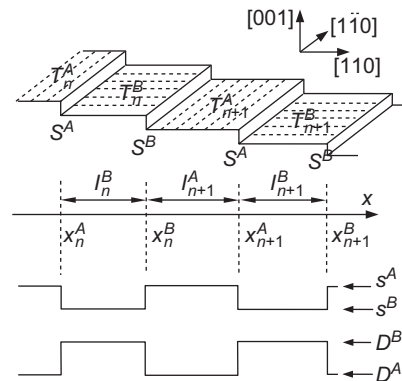

Fig. 2. A surface of silicon, vicinal to (0 0 1) and tilted towards the [1 1 0] direction, consists o two variants of terraces of the same atomic structure, except for a 90° rotation. Atoms on the terraces pair into dimers, and the rows of dimers are represented by dotted lines. Along the direction of the dimer rows, the diffusion of adatoms is fast, and the surface stress is compressive. Normal to the direction of the dimer rows, the diffusion of the adatoms is slow, and the surface stress is tensile.

consisting of alternating terraces of two variants, T^A and T^B, and alternating monatomic steps of two kinds, S^A and S^B (Chadi, 1987). The two variants of the terraces have an identical atomic structure, except for a 90° rotation; the dotted lines on each terrace represent dimer rows. The two kinds of monatomic steps, however, have dissimilar atomic structures.

When the crystal is subject to an applied strain (Men et al., 1988) or a direct electric current (Latyshev et al., 1988; Kahata and Yagi, 1989; Ichikawa and Doi, 1990; Natori et al., 1992), atoms may detach from one step, diffuse on a terrace, and attach to another step, so that some terraces may grow at the expense of others. We will only consider the case when the strain and electric current are applied along the [1 1 0] direction. The effect of the applied strain is due to the anisotropy in surface stress (Alerhand et al., 1988). Because the surface stress is compressive along the dimer rows and tensile normal to the dimer rows, a tensile strain promotes the T^B terraces, and a compressive strain promotes the T^A terraces. The effect of electric current is due to the anisotropy in diffusivity of adatoms (Latyshev et al., 1988; Stoyanov, 1990, 1992; Stoyanov et al., 1993). The electric current leads to a "wind force," motivating adatoms to diffuse in the direction of the wind, a phenomenon known as electromigration. Because adatoms diffuse faster along the dimer rows than normal to the dimer rows, adatoms predominantly diffuse on the T^B terraces. A step-down wind force relocates atoms from the S^A steps to the S^B steps, enlarging the T^B terraces. Conversely, a step-up wind force relocates atoms from the S^B steps to the S^A steps, shrinking the T^B terraces.

When the crystal is subject to both the applied strain and electric current, the two effects can act either in competition or in concert (Tamura et al., 1997). We summarize the experimental observations on a coordinate
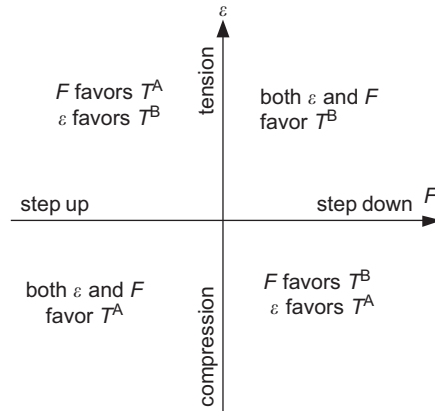
Fig. 3. Depending on the sign of the applied strain ε, and the direction of the wind force F, they can act either in concert or in competition to set a ratio of the widths of two variants of terraces.

plane spanned by the applied strain ε and the wind force F (Fig. 3). In the first quadrant, the tensile strain and the step-down wind force act in concert to enlarge T^B terraces. In the third quadrant, the compressive strain and the step-up wind force act in concert to enlarge T^A terraces. In the second and fourth quadrants, the applied strain and the wind force compete. We will show that in the second quadrant the surface will reach a stationary state, in which the relative width of the two variants of terraces becomes time-independent. In the fourth quadrant, however, we will show that the surface may undergo an instability, in which the relative width of the two variants may change drastically when experimental variables (the applied strain, the wind force, or the miscut angle) only change slightly.

2. Concentration of adatoms in equilibrium with a step

As illustrated in Fig. 2, we label terraces as ... T_n^A, T_n^B, T_{n+1}^A, T_{n+1}^B,..., and take each step to be a straight line, with steps S_n^A and S_n^B at the two ends of terrace T_n^B. Denote the positions of the two steps at time t by $x_n^A(t)$ and $x_n^B(t)$, the width of terrace T_n^A by l_n^A, and the width of terrace T_n^B by l_n^B.

Let E_a be the formation energy per adatom (i.e., the difference in energy between a crystal with an adatom and a crystal without any adatom). In this paper, we will neglect the elastic field in the crystal associated with adatoms, so that when N adatoms are on the surface, the formation energy is NE_a. This gain in energy is compensated by a gain in entropy associated with distributing a small number of adatoms to a large number of sites on the surface. In classical treatments (e.g., Pimpinelli and Villain, 1998), the tradeoff between the formation energy and the entropy gives the equilibrium concentration of adatoms.

We next consider the equilibrium concentration of adatoms in the presence of the monatomic steps. An adatom on terraces can attach to a step and becomes part of the crystal. Conversely, an atom can detach from a step and become an adatom on terraces. In these processes, the step either advances or recedes, but the overall atomic structure of the step remains invariant.

The surface energy of a crystal, Γ, depends on the applied strain in the surface, $\varepsilon_{\alpha\beta}$. Expanding the function $\Gamma(\varepsilon_{\alpha\beta})$ into a Taylor series to the first power, one writes that $\Gamma(\varepsilon_{\alpha\beta}) = \Gamma_0 + S_{\alpha\beta}\varepsilon_{\alpha\beta}$, where Γ_0 is the surface energy in the absence of the applied strain, and $S_{\alpha\beta}$ is the tensor of surface stress; see Cammarata (1994) for a review. With reference to Fig. 2, let the surface stress along the direction of the dimer rows be S^B, and that perpendicular to the dimer rows be S^A, their difference being $S = S^A - S^B$. We next examine two distinct effects of this anisotropy on the concentration of adatoms in equilibrium with a step.

First, for a crystal subject to an applied strain ε, when a S^A step moves by a unit area in the step-down direction, while all other steps remain fixed, the surface energy of the crystal increases by $S\varepsilon$. Similarly, when a S^B step moves by a unit area in the step-down direction, while all other steps remain fixed, the surface energy of the crystal decreases by $S\varepsilon$.

Second, the discontinuity in the surface stress at each step, s, induces an elastic field in the crystal. The reduction in the elastic energy in the crystal associated with a step advancing per unit area defines a driving force on the step. This force causes the steps of the same kind to attract one another, and steps of different kinds to repel one another. The magnitude of the force is $s^2(1-v)/\pi\mu l$, where μ is the shear modulus, v Poisson's ratio, and l the distance between two steps (Marchenko and Parshin, 1980; Alerhand et al., 1988; Kukta and Bhattacharya, 2002; Kukta et al., 2002).

Combining the effects of surface energy and elastic energy, we obtain the driving forces on steps S_n^A and S_n^B:

$$f_n^A = -s\varepsilon + \frac{s^2}{\pi}\frac{1-v}{\mu}\left(\sum_{m=\pm 1}^{\pm\infty}\frac{1}{x_{n+m}^A - x_n^A} - \sum_{m=-\infty}^{\pm\infty}\frac{1}{x_m^B - x_n^A}\right), \tag{1a}$$

$$f_n^B = s\varepsilon + \frac{s^2}{\pi}\frac{1-v}{\mu}\left(\sum_{m=\pm 1}^{\pm\infty}\frac{1}{x_{n+m}^B - x_n^B} - \sum_{m=-\infty}^{+\infty}\frac{1}{x_m^A - x_n^B}\right). \tag{1b}$$

The terms $\pm S\varepsilon$ are associated with the change in the surface energy caused by the applied strain ε, and the terms quadratic in s are associated with the elastic field in the crystal caused by the discontinuity in the surface stress at all steps.

The free energy of the system (i.e., the combination of the crystal, the surface, and all the adatoms) is

$$G = \int W\,\mathrm{d}V + \int \Gamma\,\mathrm{d}A + E_a N - kT[N\log N + (N_0 - N)\log(N_0 - N)]. \tag{2}$$

The first term is the elastic energy stored in the crystal, and W is the elastic energy per unit volume. The second term is the surface energy, and Γ is the surface energy per unit area. Both integrals are carried out in the undeformed configuration. The third term is the formation energy of adatoms. The fourth term is the temperature T times the entropy of distributing N adatoms to N_0 sites on the surface, and k is Boltzmann's constant. Because we take the steps to be straight, and do not allow the steps to be destroyed or created, the self-energy of the steps does not vary, and need not be included in the free energy.

When δN number of atoms detach from step x_n^A, and the step moves by δx_n^A, while all other steps are kept still, the free energy of the system varies by

$$\delta G = -f_n^A b\delta x_n^A + E_a\delta N - kT\log\left(\frac{N}{N - N_0}\right)\delta N, \tag{3}$$

where b is the thickness of the crystal in the direction along the step. Let Λ be the area per atomic site on the surface, so that $b\delta x_n^A = -\Lambda\delta N$. Setting $\delta G = 0$, we obtain the concentration of adatoms in equilibrium with step x_n^A

$$c_n^A = \exp\left(-\frac{E_a + \Lambda f_n^A}{kT}\right). \tag{4a}$$

A similar expression holds for the concentration of adatoms in equilibrium with step x_n^B

$$c_n^B = \exp\left(-\frac{E_a + \Lambda f_n^B}{kT}\right). \tag{4b}$$

Note that $\exp(-E_a/kT)$ is the equilibrium concentration of adatoms in the absence of the step–step interaction or applied strain.

3. A model that evolves terraces

On terraces, let $c(x,t)$ be the concentration of adatoms (i.e., the fraction of sites on the surface occupied by adatoms), and $J(x,t)$ be the flux of adatoms (i.e., the number of atoms crossing unit width per unit time). As reviewed by Hong et al. (2006), to attach to a S^A step, adatoms on both sides of the step must overcome excess energy barriers, known as the Erlich–Schwoebel barriers (Ehrlich and Hudda, 1966; Schwoebel and Shipsey, 1966). Due to the barrier at the step x_n^A, the concentration of adatoms on the lower terrace near the step,

$c(x_n^{A+})$, differs from the concentration of adatoms c_n^A in equilibrium with the step. Their difference, $c(x_n^{A+}) - c_n^A$, drives the attachment of adatoms to step x_n^A. Following Schwoebel (1969), we adopt a linear kinetic law, i.e., the number of atoms per length per unit time attaching to the step is given by $k_+^A[c(x_n^{A+}) - c_n^A]$, where k_+^A is the rate constant for adatoms to attach to the step from the lower terrace. Near the step x_n^A, the diffusion flux on the T^B terrace equals the rate at which adatoms attach to the step, namely

$$J(x_n^{A+}) = -k_+^A[c(x_n^{A+}) - c_n^A]. \tag{5a}$$

Similarly, the diffusion flux on the upper terrace equals the rate at which adatoms attach to the step x_n^A, namely

$$J(x_n^{A-}) = k_-^A[c(x_n^{A-}) - c_n^A], \tag{5b}$$

where k_-^A is the rate constant for the adatoms to attach to the S^A step from the upper terrace.

Both *ab initio* calculations (Zhang et al., 1995; Jeong and Oshiyama, 1999) and experimental observations (Mo and Lagally, 1991) show that there is a low or even negative barrier on both sides of S^B steps. We therefore assume that, on both sides of a S^B step, the concentration of adatoms on the terraces is in equilibrium with the step

$$c(x_n^B) = c_n^B. \tag{6}$$

Eqs. (5) and (6) establish the boundary conditions.

The flux of adatoms on terraces are driven by the gradient in the concentration of adatoms, $\partial c/\partial x$, and by the wind force F. A combination of Fick's law and Einstein's relation gives

$$J = -D\frac{\partial c}{\partial x} + \frac{cDF}{kT}, \tag{7}$$

where D is the diffusivity of adatoms, taking values D^A and D^B on the two variants of terraces.

We will focus on the case that the rate of deposition or evaporation is negligible. Furthermore, the movements of the steps are slow compared to diffusion of adatoms so that the quasi-steady state is reached, $\partial c/\partial t = 0$. Consequently, the flux J is constant on each terrace. Integrating the first-order ordinary differential Eq. (7), we obtain the distribution of the concentration

$$c(x) = C\exp\left(\frac{Fx}{kT}\right) + \frac{kTJ}{DF}, \tag{8}$$

where C is the constant of integration.

The constants C and J are specific to each terrace, and are determined by the boundary conditions at the two ends of the terrace, (Eqs. (5) and (6)). Consequently, the flux of adatoms on terrace T_n^A is

$$J_n^A = \frac{\exp\left(-\frac{E_a}{kT}\right)D^A F}{kT} \frac{\exp\left(\frac{Fl_n^A}{kT}\right)\exp\left(-\frac{\Delta f_{n-1}^B}{kT}\right) - \exp\left(-\frac{\Delta f_n^A}{kT}\right)}{\exp\left(\frac{Fl_n^A}{kT}\right) - \left(1 - \frac{FD^A}{k_-^A kT}\right)}. \tag{9a}$$

Similarly, the flux of adatoms on terrace T_n^B is

$$J_n^B = \frac{\exp\left(-\frac{E_a}{kT}\right)D^B F}{kT} \frac{\exp\left(-\frac{\Delta f_n^B}{kT}\right) - \exp\frac{Fl_n^B}{kT}\exp\left(-\frac{\Delta f_n^A}{kT}\right)}{1 - \left(\frac{FD^B}{k_+^A kT} + 1\right)\exp\frac{Fl_n^B}{kT}}. \tag{9b}$$

The difference between the fluxes from two sides of a step gives the velocity of the step. Thus

$$\frac{dx_n^A}{dt} = J_n^A - J_n^B, \tag{10a}$$

$$\frac{dx_n^B}{dt} = J_n^B - J_{n+1}^A. \tag{10b}$$

Starting from a set of initial positions of all the steps, this set of ordinary differential equations evolves $\cdots, x_{n-1}^{A}, x_{n-1}^{B}, x_{n}^{A}, x_{n}^{B}, x_{n+1}^{A}, x_{n+1}^{B}, \cdots$.

4. Stationary state

Due to the translational symmetry, the surface may reach a stationary state, in which all steps stop moving: all T^{A} terraces are of the same width l^{A}, and all T^{B} terraces are of another width l^{B}. Define an order parameter by the relative width of the two variants

$$p = \frac{l^{A} - l^{B}}{l^{A} + l^{B}}. \tag{11}$$

The parameter varies between $-1 < P < 1$. The surface is dominated by T^{A} terraces when $P < 0$, and dominated by T^{B} terraces when $P < 0$. The average width of terraces, L, equals the height of a monatomic step divided by the miscut angle. Note that $L = (l^{A} + l^{B})/2$, $l^{A} = (1 + P)L$ and $l^{B} = (1 - P)L$. The average width L, the applied strain ε, the wind force F, and the temperature T, can be controlled experimentally.

When all T^{A} terraces are of one width, and all T^{B} terraces are of another width, the driving force on every S^{A} step is the same, and the driving force on every S^{B} step is the same. The two forces, f^{A} and f^{B}, have opposite signs; (1) reduces to

$$f^{B} = -f^{A} = s\varepsilon + \frac{s^{2}}{2L}\frac{1 - v}{\mu}\tan\frac{\pi p}{2}. \tag{12}$$

In the absence of the wind force, $F = 0$, the stationary state reduces to an equilibrium state, balancing the effect of the surface energy, which favors one variant of the terraces over the other, and the elastic interaction, which causes the neighboring steps to repel each other. Setting the force on every step to zero, $f^{A} = f^{B} = 0$, we obtain that

$$\varepsilon = -\frac{s(1 - v)}{2L\mu}\tan\frac{\pi p}{2}. \tag{13}$$

This result was obtained by Alerhand et al. (1988), and was matched to the $\varepsilon - P$ relation experimentally measured by Men et al. (1988) and by Tamura et al. (1997), using $s = 1.1\,\text{N/m}$ and $\mu/(1-v) = 51\,\text{GPa}$. One may interpret this match as an experimental method to determine s.

In the presence of the wind force, $F \neq 0$, the stationary state is reached when the flux of adatoms on all terraces are the same. Eq. (9a) and Eq. (9b), we obtain the equation of stationary state

$$\varepsilon = -\frac{s(1 - v)}{2L\mu}\tan\frac{\pi p}{2}$$
$$+ \frac{kT}{\Lambda s}\log\frac{-\left(1 - \frac{D^{A}}{D^{B}}\right)\exp\left(\frac{Fl^{A}}{kT}\right) - \frac{D^{A}}{D^{B}}\exp\left(\frac{2FL}{kT}\right)\left(1 + \frac{FD^{A}}{k_{+}^{A}kT}\right) + 1 - \frac{FD^{A}}{k_{-}^{A}kT}}{\frac{D^{A}}{D^{B}} - \exp\left(\frac{2FL}{kT}\right) + \left(1 - \frac{D^{A}}{D^{B}} - \frac{FD^{A}}{k_{-}^{A}kT} - \frac{FD^{B}}{k_{+}^{A}kT}\right)\exp\left(\frac{Fl^{B}}{kT}\right)}. \tag{14}$$

This expression gives the applied strain needed to maintain a relative width p for a given wind force F, average terrace width L, and temperature T.

Write

$$D^{A} = \exp\left(-\frac{E^{A}}{kT}\right),$$

$$D^{B} = \exp\left(-\frac{E^{B}}{kT}\right),$$

$$\frac{D^{A}}{k_{-}^{A}L} = \frac{a}{L}\exp\left(\frac{E_{-}}{kT}\right),$$

$$\frac{D^{B}}{k_{+}^{A}L} = \frac{a}{L}\exp\left(\frac{E_{+}}{kT}\right). \tag{15}$$

Following Hong et al. (2006), we will use the following values: $E^A = 1\,eV$, $E^B = 0.7\,eV$, $E_- = E_+ = 0.4\,eV$, and $E_a = 1\,eV$. The distance between two neighboring atoms along the [1 1 0] direction is $a = 3.84 \times 10^{-10}\,m$, and the area per atom on the (0 0 1) surface is $\Lambda = 1.47 \times 10^{-19}\,m^2$.

We compare our model with the experiments of Tamura et al. (1997), the only experimental study on the combined effect of applied strain and electromigration. The experiments were carried out at 600 °C, with surfaces of two average terrace widths, $L = 0.13$ and $0.4\,\mu m$, and with direct electric current in either direction.
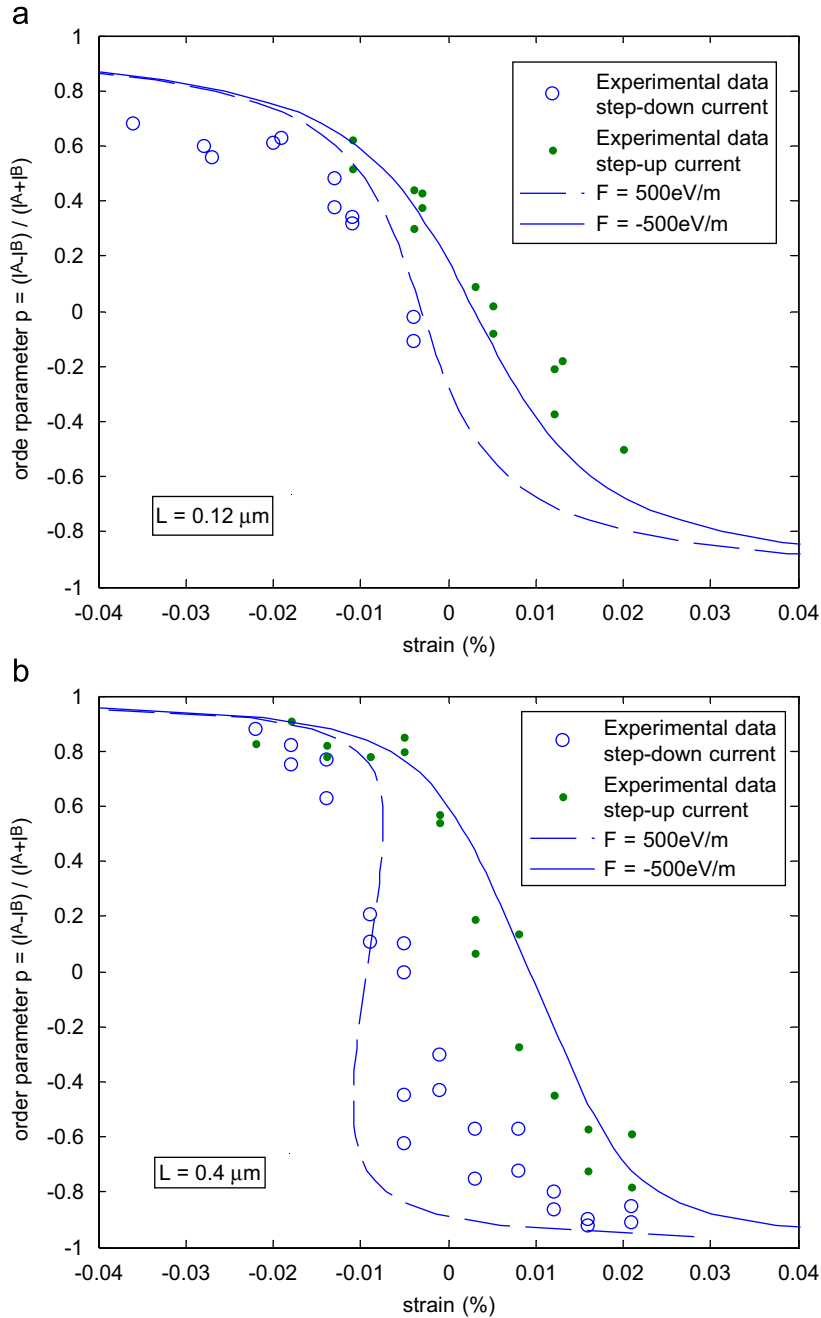

Fig. 4. In the stationary state, the relative terrace widths, $P = (l^A - l^B)/(l^A + l^B)$, is a function of the applied strain. The experimental data are taken from Tamura et al. (1997), carried out at 600 °C and electric current density of $10^6\,A/m^2$. The curves are the predictions of our model. (a) The average terrace width $L = 0.12\,\mu m$. (b) The average terrace width $L = 0.4\,\mu m$.

The current density used in the experiment was $1 \times 10^6 \, \text{Am}^{-2}$. Taking the intrinsic resistivity of silicon at 600 °C to be $1 \times 10^{-3} \, \Omega \text{m}$ (Sze, 1981), we estimate that the electric field is $E = 10^3 \, \text{V/m}$.

Fig. 4 shows the relative terrace width as a function of the applied strain. The data points are from Tamura et al. (1997), and the curves are predictions of our model. To fit our model to the four sets of experimental data, we find that the magnitude of the wind force is $F = 500 \, \text{eV/m}$. The wind force is proportional to the electric field, $F = ZeE$, where e is the magnitude of the elementary change, E is the electric field, and Z is the effective valence. The comparison between the model and experiment gives that $Z = 0.5$. This value is within the order of magnitude reported in the literature (Stoyanov, 1991; Kandel and Kaxiras, 1996).

5. Instability of stationary state

Fig. 5 plots the relative width p as a function of the applied strain ε, under various wind forces. The terrace width is $L = 0.4 \, \mu\text{m}$, and the temperature 600 °C. Under a step-up wind force, $F < 0$, p decreases as the strain increases, as expected from Fig. 3. Under a step-down wind force, $F > 0$, the wind force favors T^{B} terraces. When the step-down wind force is strong enough, p becomes a multi-valued function of ε. We will examine the physical origin of this loss of uniqueness shortly, but on the basis of Fig. 5 we expect a hysteresis loop as ε varies while holding F constant. For example, let us hold the step-down wind force at $F = 1000 \, \text{eV/m}$ and trace the curve, starting from the lower shelf where the surface is T^{B} dominant. When the applied strain is compressive and its magnitude increases to $\varepsilon \sim -0.025\%$, the surface switches to the upper shelf and becomes T^{A} dominant. As the applied strain decreases to $\varepsilon \sim -0.01\%$, the surface switches back to the lower shelf and becomes T^{B} dominant. While this instability has not been reported, the large scatter in the data of Tamura et al. (1997) at strain $\varepsilon \sim -0.005\%$, as reproduced in Fig. 4b, may as well be indicative of this instability.

To understand the origin of this instability, we simplify Eq. (14) under the following conditions. First, we assume that the process is diffusion-limited rather than attachment-limited, namely, $D^{\text{A}}/k_-^{\text{A}} L \ll 1$ and $D^{\text{B}}/k_+^{\text{A}} L \ll 1$, so that the concentration of adatoms near step S_n^{A} is in equilibrium with the step, $c(x_n^{\text{A}}) = c_n^{\text{A}}$. Second, the diffusivity along the dimer rows is much larger than that perpendicular to the dimer row, $D^{\text{B}} \gg D^{\text{A}}$, so that we neglect diffusion on T^{A} terraces and assume that $J = 0$ on all terrace in the stationary state. Under these conditions, the equation of the stationary state (14) becomes

$$\varepsilon = -\frac{s}{2L}\frac{1-v}{\mu}\tan\frac{\pi p}{2} + \frac{FL}{2\Lambda s}(p-1). \tag{16}$$

Given the numerical values for quantities in Eq. (15), the plot of Eq. (16) is almost indistinguishable from Eq. (14). Of the two terms on the right side of Eq. (16), the first is a decreasing function of p, and the second is an increasing function of p. Consequently, when F or L is large, $\varepsilon(P)$ will not be monotonic function. Equivalently, p will be a multi-valued function of the experimental variables ε, F, L.

We next examine the physical significance of the two terms on the right side of Eq.(16). The first term is due to the elastic field in the crystal and causes the neighboring steps to repel each other. When $P \to +1$ or $P \to -1$, steps form closely spaced pairs, so that the repulsion dominates. The first term also dominates when either L or F is small. When the first term dominates, the repulsion between the neighboring steps stabilizes the stationary state.

The second term in Eq. (16) is due to the wind force. When the neighboring steps are not too closely spaced, and when either F or L is large, the repulsion between steps becomes negligible, and the second term dominates (Eq. (16)). Recall that $L(1-P) = l^{\text{B}}$, when the first term in Eq. (16) is neglected, we obtain that

$$\varepsilon = -\frac{Fl^{\text{B}}}{2\Lambda s}. \tag{17}$$

Under a step-down wind ($F > 0$) and a compressive strain ($\varepsilon < 0$), corresponding to the fourth quadrant of Fig. 3, the wind force and the strain compete. On a T^{B} terrace, the compressive strain lower the equilibrium concentration of adatoms at step S^{A}, and increases the equilibrium concentration of adatoms at step S^{B}. The difference motivates adatoms to diffuse in the step-up direction, so that the compressive strain favors the T^{A} terrace. On the other hand, the wind force motivates adatoms to diffuse in the step-down direction, and favors
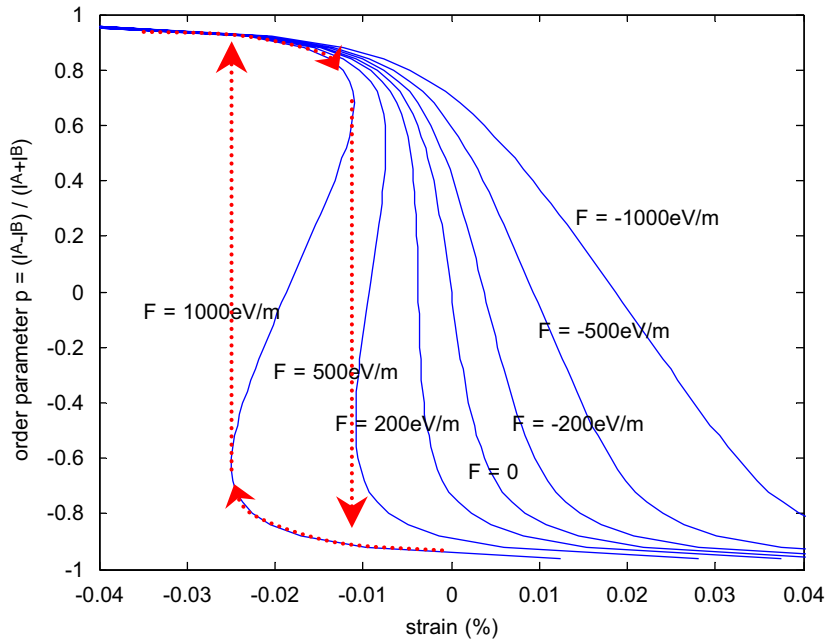
Fig. 5. The relative width of the terraces, $P = (l^A - l^B)/(l^A + l^B)$, as a function of the applied strain and the wind force. When the wind force blows step-down and is sufficiently high, e.g., $F = 1000\,eV/m$, the stationary state has an instability, in which a small change in the applied strain may lead to a large change in the relative width of the terraces. The dotted lines with arrows indicate a hysteresis loop.

the T^B terrace. The effects of the strain and the wind force balance each other to cancel the net flux of adatoms, and select the stationary width l^B.

This stationary state, however, is unstable under a step down wind force and compressive strain. The applied strain sets the equilibrium concentration of adatoms at the two steps, which in turn sets up the concentration gradient. Consequently, the applied strain is more effective in motivating the diffusion of adatoms on a narrower terrace, while the wind force is effective regardless of the width of the terrace. When l^B is larger than the stationary value, the strain is less effective in motivating diffusion, which will make l^B even larger. Conversely, when l^B is smaller than the stationary value, the strain is more effective in motivating diffusion, which will make l^B even smaller.

The same line of reasoning will show that Eq. (17) also describes the stationary state under a step-up wind and tensile strain (i.e., the second quadrant in Fig. 3). Under these conditions, the stationary state is stable: when l^B is larger than the stationary value, the strain is less effective in motivating diffusion, which will make l^B smaller.

Now return to Eq. (16). The first term stabilizes the stationary state, but the second term destabilizes the stationary state for step-down wind. Consequently, when F or L is large, the stationary state will be unstable.

Under the simplifying conditions leading to Eq. (16), temperature plays no role in this instability. Temperature, however, determines how fast this instability occurs. We simulate the dynamical process by integrating Eq. (10) directly, setting $F = 1000\,eV/m$ (step-down), $L = 0.4\,\mu m$ and $600\,°C$. Fig. 6 shows the result of one simulation, with the positions of steps as a function of time τ in units of $(L^2/D^B)\exp(E_a/kT)$, which is 6 min using the values given above. At time $\tau = 0$, all steps are equally spaced, and a strain of $\varepsilon = -0.025\%$ is applied. The surface evolves to a T^A-dominant stationary state. At time $\tau = 1000$, we change the strain to $\varepsilon = -0.015\%$, and the surface evolves to a stationary state with a slight gain in the T^B terraces. At time $\tau = 2000$, we change the strain to $\varepsilon = -0.01\%$, and the surface evolves to a T^B-dominant stationary state. The large change in the relative width associated with a small change in strain corresponds to the downward arrow from the upper shelf in Fig. 5. After an even longer time under the strain -0.01%, the stationary state becomes unstable, so that some T^B terraces grow at the expense of other T^B terraces, and multiple steps bunch.
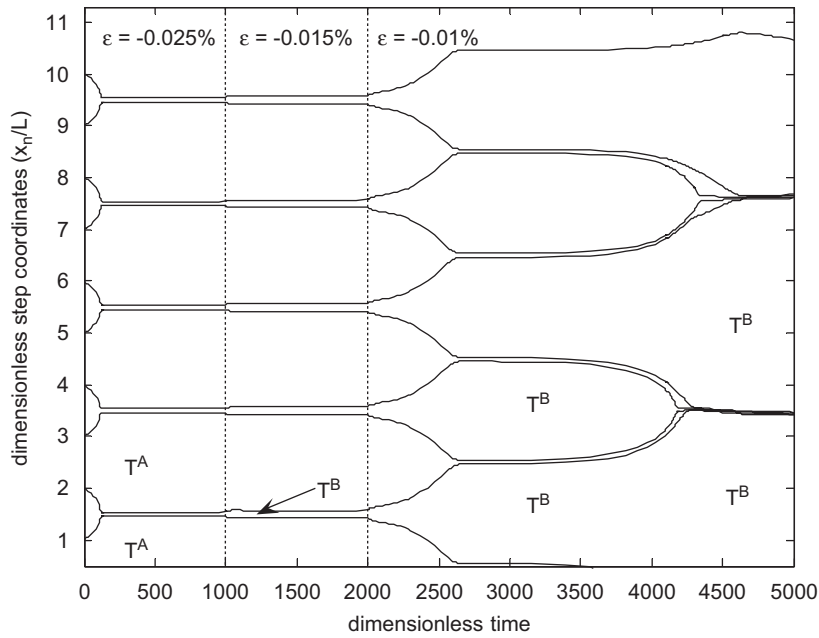
Fig. 6. Simulated evolution of terraces subject to a step-down wind force held at $F = 1000\,\text{eV/m}$ and several levels of the applied strain. At time zero, all terraces have an equal width, and the applied strain is $\varepsilon = -0.025\%$ Terraces T^A grow at the expense of terraces T^B. After the applied strain changes from -0.025% to -0.015%, T^B terraces grow slightly. However, after the applied strain changes from -0.015% to -0.01%, the surface switches to predominantly T^B terraces. After an even longer time under the strain -0.01%, the stationary state becomes unstable, so that some T^B terraces grow at the expense of other T^B terraces, and multiple steps bunch.
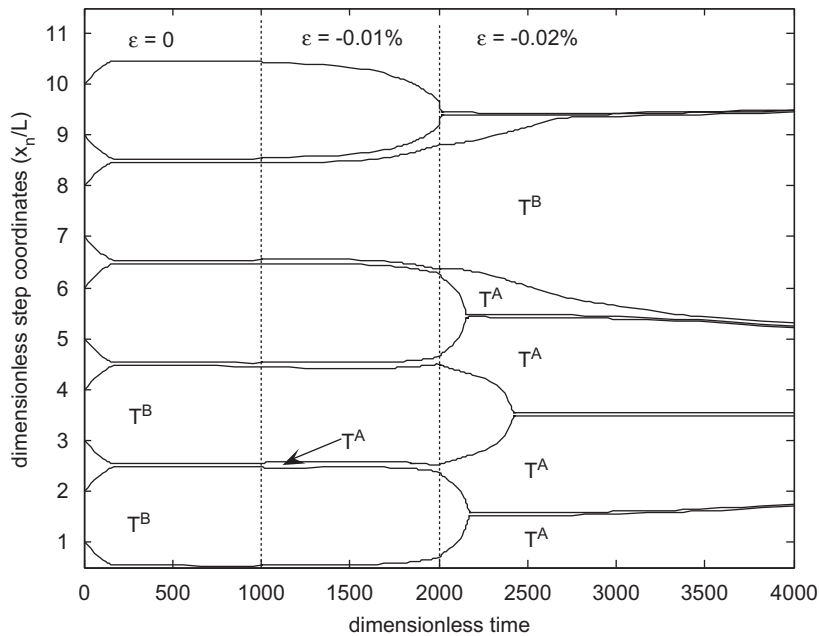

Fig. 7. Simulated evolution of terraces subject to a step-down wind force held at $F = 800\,\text{eV/m}$ and several levels of the applied strain. At time zero, all terraces have an equal width and no strain is applied. The T^B terraces grow at the expense of T^A terraces. After a strain of $\varepsilon = -0.01\%$ is applied, T^A terraces grow slightly. After the applied strain changes to -0.02%, some T^A terraces begin to grow substantially. However, before this transition is completed, steps start to bunch, so that some large T^B terraces persist.
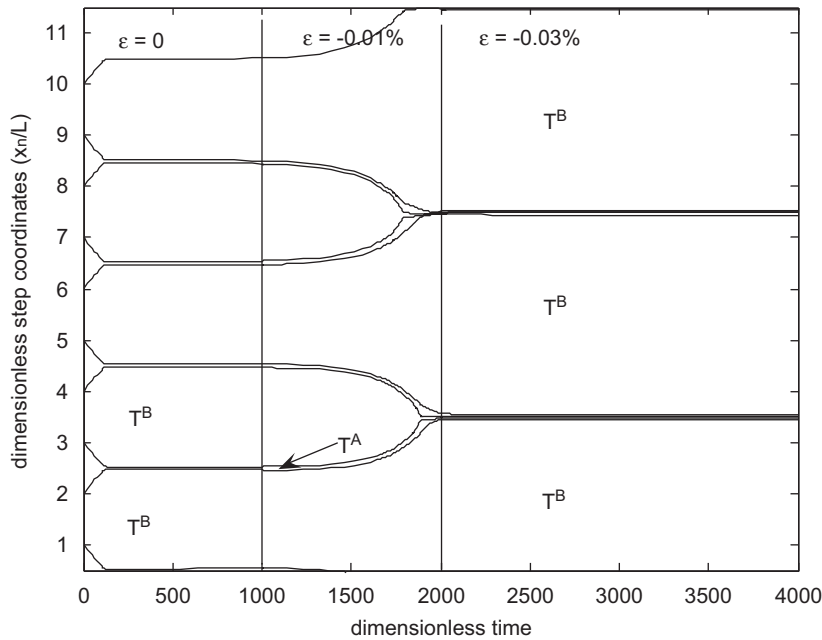
Fig. 8. Simulated evolution of terraces subject to a step-down wind force held at $F = 1000\,\mathrm{eV/m}$ and several levels of the applied strain. At time zero, all terraces have an equal width and no strain is applied. The T^B terraces grow at the expense of T^A terraces. After a strain of $\varepsilon = -0.01\%$ is applied, the relative width of the two variants of terraces changes slightly. However, steps start to bunch, so that the system is left with even larger T^B terraces separated with bunched steps. Such a bunched state is unchanged even after the applied strain is changed to $\varepsilon = -0.03\%$.

To simulate the behavior starting from the lower shelf in Fig. 5, we first prescribe a step-down wind force $F = 800\,\mathrm{eV/m}$ and zero strain (Fig. 7). The surface evolves to a stationary state dominated by T^B, as expected. At time $\tau = 1000$, we change the strain to $\varepsilon = -0.01\%$, and the surface evolves to a stationary state with a slight gain in the T^A terraces, but the surface is still dominated by T^B terraces. Meanwhile some T^B terraces begin to expand at the expense of other T^B terraces. At $\tau = 2000$, we apply a strain of $\varepsilon = -0.02\%$. Some T^A terraces start to grow, but the stationary state becomes unstable. Multiple steps start to bunch and some large T^B terraces persist.

Fig. 8 shows evolution of terraces subject to a step-down wind force held at $F = 1000\,\mathrm{eV/m}$ and several levels of the applied strain. At time zero, all terraces have an equal width and no strain is applied. The T^B terraces grow at the expense of T^A terraces. After a strain of $\varepsilon = -0.01\%$ is applied, the relative width of the two variants of terraces changes slightly. However, steps start to bunch, so that the system is left with even larger T^B terraces separated with bunched steps. Such a bunched state is unchanged even after the applied strain is changed to $\varepsilon = -0.03\%$.

Step bunching instability due to electromigration is an active field of research; see Popkov and Krug (2006), Zhao and Weeks (2005), and Thürmer et al. (1999). The above simulation has shown the interplay of the step bunching instability and the new instability discovered in this paper. A detailed study of this interplay, however, is beyond the scope of this paper.

6. Concluding remarks

We have formulated a model to evolve terraces on a vicinal silicon (0 0 1) surface under the combined action of applied strain and direct electric current. A terrace on silicon (0 0 1) surface is anisotropic. Of particular significance to this work is the anisotropy in surface stress and in diffusivity. The model incorporates the effect of the surface energy and elastic field on the concentration of adatoms at steps, and the effect of electromigration. Our model reproduces exiting experimental observations of stationary state, in which terraces of two variants maintain a constant relative width. Our model also predicts a new instability, in which

a small change in the control parameters (i.e., the applied strain, the wind force, and the average terrace width) may lead to a large change in the order parameter (i.e., the ratio of the terraces of two variants). This finding calls for new experimental study.

Acknowledgements

References

Alerhand, O.L., Vanderbilt, D., Meade, R.D., Joannopoulos, J.D., 1988. Spontaneous formation of stress domains on crystal surfaces. Phys. Rev. Lett. 61 (17), 1973–1976.

Burton, W.K., Cabrera, N., Frank, F.C., 1951. The growth of crystals and the equilibrium structure of their surfaces. Philos. Trans. R. Soc. London Ser. A Math. Phys. Sci. 243 (866), 299–358.

Cammarata, R.C., 1994. Surface and interface stress effects in thin films. Progr. Surf. Sci. 46 (1), 1–38.

Chadi, D.J., 1987. Stabilities of single-layer and bilayer steps on Si(0 0 1) surfaces. Phys. Rev. Lett. 59 (15), 1691–1694.

Ehrlich, G., Hudda, F.G., 1966. Atomic view of surface self-diffusion-tungsten on tungsten. J. Chem. Phys. 44 (3), 1039–1049.

Hong, W., Zhang, Z.-Y., Suo, Z., 2006. Interplay between elastic interactions and kinetic processes in stepped Si (0 0 1) homoepitaxy. Phys. Rev. B, 74 (23), 235318.

Ichikawa, M., Doi, T., 1990. Observation of electromigration effect upon Si-MBE growth on Si(0 0 1) surface. Vacuum 41 (4–6), 933–937.

Jeong, S., Oshiyama, A., 1999. Complex diffusion mechanisms of a silicon adatom on hydrogenated Si(1 0 0) surfaces: on terraces and near steps. Surf. Sci. 433–435, 481–485.

Jeong, H.-C., Williams, E.D., 1999. Steps on surfaces: experiment and theory. Surf. Sci. Rep. 34 (6–8), 175–294.

Kahata, H., Yagi, K., 1989. REM observation on conversion between single-domain surfaces of Si(001) 2×1 and 1×2 induced by specimen heating current. Jpn. J. Appl. Phys. 2—Lett. 28 (5), L858–L861.

Kandel, D., Kaxiras, E., 1996. Microscopic theory of electromigration on semiconductor surfaces. Phys. Rev. Lett. 76 (7), 1114–1117.

Kukta, R.V., Bhattacharya, K., 2002. A micromechanical model of surface steps. J. Mech. Phys. Solids 50 (3), 615–649.

Kukta, R.V., Peralta, A., Kouris, D., 2002. Elastic interaction of surface steps: effect of atomic-scale roughness. Phys. Rev. Lett. 88 (18), 186102.

Latyshev, A.V., Krasil'nikov, A.B., Aseev, A.L., Stenin, S.I., 1988. Effect of electric current on the ratio of the areas of the (2×1) and (1×2) domains at the clean (0 0 1) surface of silicon during sublimation. JETP Lett. 48 (9), 526–529.

Marchenko, V.I., Parshin, A.Y., 1980. On the elastic property of crystal-surfaces. Zh. Eksp. Teor. Fiz. 79 (1), 257–260.

Men, F.K., Packard, W.E., Webb, M.B., 1988. Si(1 0 0) surface under an externally applied stress. Phys. Rev. Lett. 61 (21), 2469–2471.

Mo, Y.W., Lagally, M.G., 1991. Anisotropy in surface migration of Si and Ge on Si(001). Surf. Sci. 248 (3), 313–320.

Natori, A., Fujimura, H., Fukuda, M., 1992. Step structure transformation of Si(0 0 1) surface induced by current II. Appl. Surf. Sci. 60–61, 85–91.

Pimpinelli, A., Villain, J., 1998. Physics of Crystal Growth. Cambridge University Press, Cambridge.

Popkov, V., Krug, J., 2006. Dynamic phase transitions in electromigration-induced step bunching. Phys. Rev. B 73 (23), 235430.

Schwoebel, R.L., Shipsey, E.J., 1966. Step motion on crystal surfaces. J. Appl. Phys. 37 (10), 3682–3686.

Schwoebel, R.L., 1969. Step motion on crystal surfaces. II. J. Appl. Phys. 40 (2), 614–618.

Stoyanov, S., 1990. Formation of bilayer steps during growth and evaporation of Si(0 0 1) vicinal surfaces. Europhys. Lett. 11 (4), 361–366.

Stoyanov, S., 1991. Electromigration induced step bunching on Si surfaces—How does it depend on the temperature and heating current direction. Jpn. J. Appl. Phys. 30 (1), 1–6.

Stoyanov, S., 1992. New development in the theory of MBE growth of Si-a confrontation with experiment. Appl. Surf. Sci. 60–61, 55–63.

Stoyanov, S., Ichikawa, M., Doi, T., 1993. High-temperature MBE growth of Si-direct-current heating effects on (1 1 1) and (0 0 1) vicinal surfaces. Jpn. J. Appl. Phys. 1—Regular Papers Short Notes Rev Papers 32 (5A), 2047–2051.

Sze, S.M., 1981. Physics of Semiconductor Devices, second ed. Wiley, New York.

Tamura, H., Tanishiro, Y., Minoda, H., Yagi, K., 1997. Competing effects of current and strain on step structures on Si(001)2×1 studied by REM. Surf. Sci. 382 (1–3), 310–319.

Thürmer, K., Liu, D.-J., Weeks, J.D., Williams, E.D., 1999. Onset of step anti-banding instability due to surface electromigration. Phys. Rev. Lett. 83, 5531.

Zhang, Z.-Y., Lagally, M.G., 1997. Atomistic processes in the early stages of thin-film growth Science 276, 377–383.

Zhang, Q.-M., Roland, C., Boguslawski, P., Bernholc, J., 1995. *Ab initio* studies of the diffusion barriers at single-height Si(1 0 0) steps. Phys. Rev. Lett. 75 (1), 101–104.

Zhao, T., Weeks, J.D., 2005. A two-region diffusion model for current-induced instabilities of step patterns on vicinal Si (1 1 1) surfaces. Surf. Sci. 580 (1–3), 107–121.